Eur. Phys. J. C 51, 569–583 (2007)
DOI 10.1140/epjc/s10052-007-0316-5

THE EUROPEAN PHYSICAL JOURNAL C

Regular Article – Theoretical Physics

Scalar QED, NLO and PHOTOS Monte Carlo[a]

G. Nanava[1,b], Z. Wąs[1,2]

[1] Institute of Nuclear Physics, PAN, Kraków, ul. Radzikowskiego 152, Poland
[2] CERN, 1211 Geneva 23, Switzerland

Received: 28 February 2007 /
Published online: 17 May 2007 –

Abstract. Recently, QED bremsstrahlung in B meson decays into pair of scalars (πs and/or Ks) has become of interest. If experimental acceptance must be taken into account, the PHOTOS Monte Carlo technique is often used in experimental simulations. We will use scalar QED to benchmark PHOTOS, even though this theory is of limited use for complex objects. We present the analytical form of the kernel used in the older versions of PHOTOS, and the new, exact (scalar QED) one. Matrix element and phase-space Jacobians are separated in the final weight, and future extensions based on measurable electromagnetic form-factors are thus possible. The massive phase-space is controlled in the program with no approximations. Thanks to the iterative solution, all leading and next to leading logarithmic terms are properly reproduced by the Monte Carlo simulation. Simultaneously, full differential distributions over the complete multiple-body phase-space are provided. An agreement of better than 0.01% with independent calculations of scalar QED is demonstrated.

PACS. 13.20.He; 13.40.Ks

1 Introduction

In the analysis of data from high-energy physics experiments, one tries to resolve the "*experiment = theory*" equation. This non-trivial task requires that a lot of different effects be considered simultaneously. From the experimental side, these are mainly detector acceptance and cuts, which are dictated by the construction and physical properties of the detector. The shapes of the distributions may be distorted by, say, misidentification and residual background contamination. These effects need to be discriminated in an appropriate and well-controlled way. From the theoretical side, *all* effects of known physics have to be included in the predictions as well. Only then the experimental data and theoretical predictions can be confronted to determine the numerical values of the coupling constants or the effects of new physics (to be discovered).

A well-defined class of theoretical effects consists of QED radiative corrections. PHOTOS is a universal Monte Carlo algorithm that simulates the effects of QED radiative corrections in decays of particles and resonances. It is a project with a rather long history: the first version was released in 1991 [1], followed by version 2.0 [2] (double emission and threshold terms for fermions). The package is in wide use [3]; it was applied as a precision simulation tool for the W mass measurement at the Tevatron [4] and LEP [5, 6], and for CKM matrix measurements in the decays of K and B resonances (NA48 [7], KTeV [8], Belle [9], BaBar [10] and Fermilab [11]). Discussion of the different components of the systematic errors in PHOTOS is thus of interest.

Throughout the years the core algorithm for the generation of $O(\alpha)$ corrections did not change much; however, its precision, applicability to various processes, and numerical stability improved significantly. New functionalities, such as multiple photon radiation and interference effects for all possible decays, were introduced [12, 13]. Recently, the complete first order matrix element was introduced into PHOTOS for Z decays and complete NLO[1] multiple

[a] Supported in part by the EU grant MTKD-CT-2004-510126, in partnership with the CERN Physics Department, and the Polish State Committee for Scientific Research (KBN) grant 2 P03B 091 27 for the years 2004–2006.
This work is partly supported by the EU grant mTkd-CT-2004-510126 in partnership with the CERN Physics Department and by the Polish Ministry of Scientific Research and Information Technology grant No. 620/E-77/6.PRUE/DIE 188/2005-2008

[b] e-mail: Gizo.Nanava@ifj.edu.pl
On leave from IHEP, TSU, Tbilisi, Georgia

[1] In the paper, we will use the abbreviations NLO, NLL, NNLO, NNLL to denote next to leading order, next to leading logarithm, next to next to leading order, next to next to leading logarithm corrections with respect to leading order (that is, without QED at all). The meaning for such abbreviations cannot be defined restrictively on the basis of approximations used in phase-space. The properties of the matrix elements need to be specified as well. Nonetheless, we will use the abbreviations later in the paper to denote such approximations in the phase-space Jacobians, which do not prevent the appropriate precision from holding if a proper choice of the matrix elements is made as well.

photon predictions for that channel were demonstrated to work well [14].

Increasing interest in the algorithm expressed by experimental collaborations (including future LHC experiments and precise measurements for B decays) was a motivation to perform a more detailed study of the potential and precision of the PHOTOS algorithm. This paper is devoted to the decay of B mesons into a pair of scalars. It is a continuation of the previous paper [14], devoted to Z decays. We concentrate our attention on the exact phase-space parametrization as used in PHOTOS, and on the explicit separation of the final weight into parts responsible for the following:(i) *mass dependent* phase-space Jacobians, (ii) matrix elements and (iii) presampler for peaks.

Simplifications introduced in the matrix element normally used in these scalar B meson decays are removed, and the exact kernel of the first order scalar QED calculation is installed. Such an improvement opens the way to the inclusion of data dependent form-factors into the matrix elements of PHOTOS and to physically better results than of scalar QED alone.

Our study of the PHOTOS algorithm can be understood as another step in the on-going effort to find practical solutions of the improved expansions. The solution can be seen as a rearrangement of the QED perturbation expansion, but this time for the interaction of charged scalars with photons and in the case in which ultrarelativistic approximations are not valid.

To test PHOTOS we have used predictions of the SANC [15] Monte Carlo algorithm. SANC is able to calculate the exact first order scalar QED matrix elements for decays of B mesons into scalars, and it covers the full phase-space of the decay products without any approximations. Events provided by SANC MC are unweighted. SANC is a network client-server system for the semi-automatic calculation of electroweak, QCD and QED radiative corrections at one-loop precision level for various processes (decays) of elementary particle interactions.

The paper is organized as follows. Section 2 is devoted to the description of our results obtained from scalar QED, which will be used later in tests and in the construction of the kernel for single photon emission. In Sect. 3 the main properties used in the design of PHOTOS are presented. In particular, the construction of the weight (NLO level) necessary to introduce the complete first order matrix element is explained in full detail. The phase-space parametrization used in the iterative solution of PHOTOS is given. Details are collected in the appendix. On the other hand, aspects of the construction, quite essential for complete NLL, will still remain poorly documented. The issue is how the parts of the single photon emission matrix element are used in the kernel (iterated and thus extended to multiphoton emissions). Section 4 is devoted to the results of numerical tests performed at fixed, first order of QED. Some numerical results obtained with the multiphoton version of the program will be collected there for reference. Finally, Sect. 5 summarizes the paper.

2 Scalar QED and B decays

In this section we give the formulae needed in the construction of the Monte Carlo routine of two-particle B meson decays and the analytical results of the decay rates at $\mathcal{O}(\alpha)$ in scalar QED when the masses of the decay products are neglected. The one-loop QED corrections to the width of the decays $B^{0,-} \to H_1^- H_2^{+,0}$, where $H_{1,2}$ denotes scalar (pseudo-scalar) particles, can be represented as a sum of the Born contribution and the contributions due to virtual loop diagrams and soft and hard photon emissions. Both virtual and soft contributions factorize to the Born one. We have

$$\mathrm{d}\Gamma^{\mathrm{Total}} = \mathrm{d}\Gamma^{\mathrm{Born}} \left[1 + \frac{\alpha}{\pi}\left(\delta^{\mathrm{soft}} + \delta^{\mathrm{virt}}\right)\right] + \mathrm{d}\Gamma^{\mathrm{Hard}}\,. \tag{1}$$

Here $\mathrm{d}\Gamma^{\mathrm{Born}}$ is the tree level differential decay width, δ^{virt} represents the virtual corrections, δ^{soft} denotes the soft photon contribution, and $\mathrm{d}\Gamma^{\mathrm{Hard}}$ is the hard photon contribution. The Born level distribution in the rest frame of the decaying meson can be written as

$$\mathrm{d}\Gamma^{\mathrm{Born}} = \frac{1}{2\,M}\left|A^{\mathrm{Born}}\right|^2 \mathrm{dLips}_2(P \to k_1, k_2)\,, \tag{2}$$

where M is the mass of the decaying particle, $k_{1,2}$ denote the momenta of the decay products, A^{Born} stands for the corresponding tree level amplitude, and $\mathrm{dLips}_2(P \to k_1, k_2)$ is the two-body differential phase-space. For the latter we choose the following parametrization:

$$\begin{aligned}&\mathrm{dLips}_2(P \to k_1, k_2)\\ &= \frac{1}{32\pi^2}\frac{\lambda^{1/2}(M^2, m_1^2, m_2^2)}{M^2}\,\mathrm{d}\cos\theta_1\,\mathrm{d}\phi_1\,,\end{aligned} \tag{3}$$

where the angles θ_1 and ϕ_1 define the orientation of the momentum k_1 in the rest frame of the B meson. As usual we define $\lambda^{\frac{1}{2}}(a,b,c) = \sqrt{a^2+b^2+c^2-2ab-2ac-2bc}$. In the case of neutral B meson decay channels, $B^0 \to H_1^- H_2^+$, the scalar QED calculations for the virtual and soft factors in (1) give

$$\begin{aligned}\delta^{\mathrm{virt}} = &\left[1 + \frac{M^2-m_1^2-m_2^2}{\Lambda}\ln\frac{2m_1m_2}{M^2-m_1^2-m_2^2+\Lambda}\right]\ln\frac{M^2}{m_\gamma^2}\\ &+\frac{3}{2}\ln\frac{\mu_{\mathrm{UV}}^2}{M^2} + \frac{M^2-m_1^2-m_2^2}{2\Lambda}\\ &\times\left[\mathrm{Li}_2\left(\frac{M^2+m_1^2-m_2^2+\Lambda}{2\Lambda}\right)\right.\\ &\quad-\mathrm{Li}_2\left(\frac{M^2+m_1^2-m_2^2-\Lambda}{-2\Lambda}\right)\\ &\quad+2\ln\frac{2Mm_1}{M^2+m_1^2-m_2^2+\Lambda}\ln\frac{m_1\Lambda}{M^3}\\ &\quad\left.+(1\leftrightarrow 2)+\pi^2\right]\\ &-\frac{\Lambda}{2M^2}\ln\frac{2m_1m_2}{M^2-m_1^2-m_2^2+\Lambda} + \frac{m_2^2-m_1^2}{4M^2}\ln\frac{m_2^2}{m_1^2}\\ &-\frac{1}{2}\ln\frac{m_1m_2}{M^2}+1\,,\end{aligned} \tag{4}$$

$$\delta^{\rm soft} = \left[1+\frac{M^2-m_1^2-m_2^2}{\Lambda}\ln\frac{2m_1m_2}{M^2-m_1^2-m_2^2+\Lambda}\right]\ln\frac{m_\gamma^2}{4\omega^2} + \frac{M^2-m_1^2-m_2^2}{2\Lambda}\left[{\rm Li}_2\left(\frac{-2\Lambda}{M^2+m_1^2-m_2^2-\Lambda}\right) - {\rm Li}_2\left(\frac{2\Lambda}{M^2+m_1^2-m_2^2+\Lambda}\right)+(1\leftrightarrow 2)\right] - \frac{M^2+m_1^2-m_2^2}{\Lambda}\ln\frac{2Mm_1}{M^2+m_1^2-m_2^2+\Lambda} - (1\leftrightarrow 2)\,, \tag{5}$$

where $m_{1,2}$ are the final meson masses, an auxiliary small parameter $\omega \ll M/2$ separates the soft and hard photon contributions, and $\mu_{\rm UV}$ denotes the ultraviolet scale. An auxiliary photon mass m_γ is used as a regulator of the infrared divergences. The ultraviolet singularities are regularized by means of dimensional regularization. We renormalize the wave functions of the external scalar fields in the on-shell scheme and for point-like weak coupling in the $\overline{\rm MS}$ scheme. We have $\Lambda = \lambda^{1/2}(M^2,m_1^2,m_2^2)$ and ${\rm Li}_2(z) = -\int_0^z \frac{{\rm d}y}{y}\ln|1-y|$.

The hard photon distribution ${\rm d}\Gamma^{\rm Hard}$ in scalar QED can be expressed as follows:

$${\rm d}\Gamma^{\rm Hard} = \frac{1}{2\,M}|A^{\rm Born}|^2 4\pi\alpha\left(q_1\frac{k_1.\epsilon}{k_1.k_\gamma}-q_2\frac{k_2.\epsilon}{k_2.k_\gamma}\right)^2 \times {\rm dLips}_3(P\to k_1,k_2,k_\gamma)\,. \tag{6}$$

Here, $q_{1,2}$ are the charges of the final mesons, and k_γ and ϵ_μ are the photon momentum and polarization vector, respectively. The three-body differential phase-space of the decay products, ${\rm dLips}_3(P\to k_1,k_2,k_\gamma)$, is parametrized, in a rather standard way (see e.g. [16]), as follows:

$$\begin{aligned}&{\rm dLips}_3(P\to k_1,k_2,k_\gamma)\\ &= \frac{\lambda^{1/2}(1-2E_\gamma/M, m_1^2/M^2, m_2^2/M^2)}{16(2\pi)^5(1-2E_\gamma/M)}\\ &\quad\times E_\gamma\,{\rm d}E_\gamma\,{\rm d}\cos\theta_\gamma\,{\rm d}\phi_\gamma\,{\rm d}\cos\theta_1^R\,{\rm d}\phi_1^R\,,\end{aligned} \tag{7}$$

where the angles θ_1^R and ϕ_1^R define the orientation of the momentum k_1 in the rest frame of (k_1+k_2); the photon energy E_γ and the angles θ_γ and ϕ_γ, which define the orientation of the photon momentum, are given in the rest frame of the decaying particle. These parameters vary in the limits $0\le\theta_\gamma,\ \theta_1^R\le\pi$, $0\le\phi_\gamma,\ \phi_1^R\le 2\pi$ and $\omega\le E_\gamma\le(M^2-(m_1+m_2)^2)/2M$. Equations (1)–(7) are used in the construction of the Monte Carlo simulator of the decays under consideration. An analytical integration in (6) over the phase-space variables (7) can easily be done. Below we give the result of integration in the massless limit of the final mesons (i.e. $m_1,m_2\equiv m\to 0$), because of its simplicity,

$$\Gamma^{\rm Hard} = \Gamma^{\rm Born}\frac{\alpha}{\pi}\left[\left(1+\ln\frac{m^2}{M^2}\right)\ln\frac{4\omega^2}{M^2}+\ln\frac{m^4}{M^4}-\frac{\pi^2}{3}+4\right]. \tag{8}$$

The virtual correction depends on the ultraviolet scale $\mu_{\rm UV}$, which should cancel in the total decay width, because of the scale dependence of the point-like weak coupling. The infrared divergence cancels in the sum of virtual and soft contributions, as it must. The total decay width, which is the sum of the contributions (4), (5), and (8), is also free of ω and of the final meson mass singularity in accordance with the KLN theorem [17]–[18]:

$$\Gamma^{\rm Total} = \Gamma^{\rm Born}\left[1+\frac{\alpha}{\pi}\left(\frac{3}{2}\ln\frac{\mu_{\rm UV}^2}{M^2}+5\right)\right]. \tag{9}$$

The same calculations can be done for the charged B meson decay channels $B^-\to H_1^-H_2^0$. In this case, for the various contributions in (1), we obtain

– a virtual photon contribution,

$$\begin{aligned}\delta^{\rm virt} =& \left[1+\frac{M^2+m_1^2-m_2^2}{\Lambda}\ln\frac{2Mm_1}{M^2+m_1^2-m_2^2+\Lambda}\right]\ln\frac{Mm_1}{m_\gamma^2}\\ &+\frac{M^2+m_1^2-m_2^2}{2\Lambda}\left[{\rm Li}_2\left(\frac{M^2-m_1^2-m_2^2+\Lambda}{2\Lambda}\right)\right.\\ &-{\rm Li}_2\left(\frac{M^2-m_1^2-m_2^2-\Lambda}{-2\Lambda}\right)\\ &+{\rm Li}_2\left(\frac{M^2+m_2^2-m_1^2-\Lambda}{-2\Lambda}\right)\\ &-{\rm Li}_2\left(\frac{M^2+m_2^2-m_1^2+\Lambda}{2\Lambda}\right)\\ &+2\ln\frac{2Mm_1}{M^2+m_1^2-m_2^2+\Lambda}\ln\frac{\Lambda}{Mm_2}\\ &\left.-\ln\frac{2Mm_2}{M^2+m_2^2-m_1^2+\Lambda}\ln\frac{M^2}{m_1^2}\right]+\frac{3}{2}\ln\frac{\mu_{\rm UV}^2}{Mm_1}\\ &+\frac{\Lambda}{2m_2^2}\ln\frac{2Mm_1}{M^2+m_1^2-m_2^2+\Lambda}\\ &-\frac{M^2-m_1^2}{4m_2^2}\ln\frac{m_1^2}{M^2}+1\,;\end{aligned} \tag{10}$$

– a soft photon contribution,

$$\begin{aligned}\delta^{\rm soft} =& \left[1+\frac{M^2+m_1^2-m_2^2}{\Lambda}\ln\frac{2Mm_1}{M^2+m_1^2-m_2^2+\Lambda}\right]\ln\frac{m_\gamma^2}{4\omega^2}\\ &+\frac{M^2+m_1^2-m_2^2}{2\Lambda}\left[{\rm Li}_2\left(\frac{-2\Lambda}{M^2+m_1^2-m_2^2-\Lambda}\right)\right.\\ &\left.-{\rm Li}_2\left(\frac{2\Lambda}{M^2+m_1^2-m_2^2+\Lambda}\right)\right]\\ &-\frac{M^2+m_1^2-m_2^2}{\Lambda}\ln\frac{2Mm_1}{M^2+m_1^2-m_2^2+\Lambda}+1\,;\end{aligned} \tag{11}$$

– and a hard photon contribution,

$$\begin{aligned}{\rm d}\Gamma^{\rm Hard} =& \frac{1}{2\,M}|A^{\rm Born}|^2 4\pi\alpha\left(q_1\frac{k_1.\epsilon}{k_1.k_\gamma}-q\frac{P.\epsilon}{P.k_\gamma}\right)^2\\ &\times{\rm dLips}_3(P\to k_1,k_2,k_\gamma)\,,\end{aligned}$$

$$\begin{aligned}\Gamma^{\rm Hard} =& \Gamma^{\rm Born}\frac{\alpha}{\pi}\left[\left(1+\ln\frac{m}{M}\right)\ln\frac{4\omega^2}{M^2}\right.\\ &\left.+\ln\frac{m^2}{M^2}-\frac{\pi^2}{6}+3\right].\end{aligned} \tag{12}$$

Table 1. Comparison of the B-meson total decay widths produced by analytical calculations (second column) and by Monte Carlo (third column). The last significant digit of the Monte Carlo results is given in brackets

Channel	$\Gamma^{\rm Total}_{\rm AC}$, 10^{-3} MeV	$\Gamma^{\rm Total}_{\rm MC}$, 10^{-3} MeV
$B^- \to \pi^-\pi^0$	0.373629	0.3736(4)
$B^- \to K^-K^0$	0.367586	0.3675(9)
$B^0 \to \pi^-\pi^+$	0.377392	0.3773(8)
$B^0 \to K^-K^+$	0.371414	0.3714(2)

Again after integration over the phase-space variables, the massless limit of the final mesons (i.e. $m_1, m_2 \equiv m \to 0$) was used in the previous formula. Finally, summing the contributions (10)–(12), we obtain the following expression for the total decay width:

$$\Gamma^{\rm Total} = \Gamma^{\rm Born}\left[1+\frac{\alpha}{\pi}\left(\frac{3}{2}\ln\frac{\mu^2_{\rm UV}}{M^2}-\frac{\pi^2}{3}+\frac{11}{2}\right)\right]. \tag{13}$$

We have checked that the factors $\delta^{\rm soft}$ and $\delta^{\rm virt}$ in (1), for both charged and neutral B meson decays, provide the same numerical results as the corresponding expressions in [19].

To be assured of the accuracy of the SANC Monte Carlo integration (which is a byproduct of the MC simulation), we compared the Monte Carlo results with the analytical calculations of the total decay rate. The result of this comparison is shown in Table 1[2]. The agreement is thus better than 10^{-4} in this test, in which mass effects had been included.

3 Exact phase-space and matrix element

To start any discussion of the implementation of complete first order QED radiative corrections in B decay, one has to specify the parametrization of the complete phase-space slots of the fixed final-state multiplicity.

Let us start with the explicit expression for the parametrization of an $n+1$-body phase-space in the decay of the object of four-momentum P ($P^2 = M^2$), as used in PHOTOS Monte Carlo. As our aim is to define iterative relations, let us denote the four-momenta of the first n decay products as k_i ($i = 1, n$) and the last $n+1$ decay product as k_{n+1}. In our case the $n+1$th particle will always be the real and massless photon[3]. In the latter steps of our construction the masslessness of the photons and the properties of the QED matrix elements will be used.

In the following, the notation from [20, 21] will be used. We will not rely on any particular results of these papers. We only point out other, similar options for the exact n-body phase-space parametrizations, which are also in use.

The Lorentz invariant phase-space is defined as follows:

$$\begin{aligned}
&{\rm dLips}_{n+1}(P)\\
&= \frac{{\rm d}^3k_1}{2k^0_1(2\pi)^3}\cdots\frac{{\rm d}^3k_n}{2k^0_n(2\pi)^3}\frac{{\rm d}^3k_{n+1}}{2k^0_{n+1}(2\pi)^3}\\
&\quad\times(2\pi)^4\delta^4\left(P-k_{n+1}-\sum_{i=1}^{n}k_i\right)\\
&= {\rm d}^4p\,\delta^4(P-p-k_{n+1})\frac{{\rm d}^3k_{n+1}}{2k^0_{n+1}(2\pi)^3}\\
&\quad\times\frac{{\rm d}^3k_1}{2k^0_1(2\pi)^3}\cdots\frac{{\rm d}^3k_n}{2k^0_n(2\pi)^3}(2\pi)^4\delta^4\left(p-\sum_{i=1}^{n}k_i\right)\\
&= {\rm d}^4p\,\delta^4(P-p-k_{n+1})\frac{{\rm d}^3k_{n+1}}{2k^0_{n+1}(2\pi)^3}\\
&\quad\times{\rm dLips}_n(p\to k_1\ldots k_n)\,,
\end{aligned}\tag{14}$$

where extra integration variables and the four-vector p (compensated with $\delta^4(p-\sum_1^n k_i)$) are introduced. If further $M_{1\ldots n}$ (compensated with $\delta(p^2-M^2_{1\ldots n})$) is introduced, the element of the phase-space takes the form

$$\begin{aligned}
&{\rm dLips}_{n+1}(P)\\
&= \frac{{\rm d}M^2_{1\ldots n}}{(2\pi)}\,{\rm dLips}_2(P\to p\;k_{n+1})\,{\rm dLips}_n(p\to k_1\ldots k_n)\\
&= {\rm d}M^2_{1\ldots n}\left[{\rm d}\cos\hat\theta\,{\rm d}\hat\phi\frac{1}{8(2\pi)^3}\frac{\lambda^{\frac12}\left(M^2,M^2_{1\ldots n},m^2_{n+1}\right)}{M^2}\right]\\
&\quad\times{\rm dLips}_n(p\to k_1\ldots k_n)\,.
\end{aligned}\tag{15}$$

The part of the phase-space Jacobian corresponding to integration over the direction and energy of the last particle (or equivalently the invariant mass $M_{1\ldots n}$ of the remaining system of $1\ldots n$ particles) is explicitly given. We will use later in the formulas $m^2_i = k^2_i$, and analogously $M_{i\ldots n}$, defining the invariant masses of the $k_i\ldots k_n$ systems. The integration over the angles $\hat\theta$ and $\hat\phi$ is defined in the P rest frame. The integration over the invariant mass, $M_{1\ldots n}$, is limited by phase-space boundaries. Anybody familiar with the phase-space parametrization as used in FOWL [16], TAUOLA [21], or in many other programs will find the above explanation quite standard[4].

The question of the choice of axes with respect to which angles are defined and of the order in the kinematical construction is less trivial. The choice for the particular option stems from the necessity to presample collinear singularities. It is rather well known that the choice of the reference directions for the parametrization of the unit sphere is free,

[2] Please note that these numbers are for the purpose of our test only; the overall B–H–H coupling constants do not match the experimental data.

[3] However the construction does not rely on a photon to be massless. In principle it can be applied to define other phase-space relations, for example the emission of an extra massive pion or emission of a pair of heavy particles.

[4] The parametrizations of such a type use the properties of the Lorentz group in an explicit manner, in particular the measure, representations and their products. That is why they are useful for event building Monte Carlo programs in phase-space constructions based on boosts and rotations.

and that it can be used to advantage. We will use a related, but somewhat different freedom of choice. Instead of the variables $\hat{\theta}$ and $\hat{\phi}$ defining the orientation of k_{n+1} in the P rest frame we will use the angles θ_1 and ϕ_1 orienting k_1 (also in the P rest frame). The Jacobian for this reparametrization of the unit sphere equals 1 as well[5].

Equation (15) can be iterated and provides a parametrization of the phase-space with an arbitrary number of final-state particles. In such a case, the question of the orientation of the frames used to define the angles and the order of the $M_{i\ldots n}$ integrations (consequently, the choice of the limits for the $M_{i\ldots n}$ integration) becomes particularly rich. Our choice is defined in [2]. We will not elaborate on this point here; nothing new was introduced for the purpose of our study.

If the invariant mass $M_{1\ldots n}$ is replaced with the photon energy defined in the P rest frame, k_γ, then the phase-space formula can be written as

$$\begin{aligned}&\mathrm{dLips}_{n+1}(P)\\&=\left[k_\gamma\,\mathrm{d}k_\gamma\,\mathrm{d}\cos\hat{\theta}\,\mathrm{d}\hat{\phi}\frac{1}{2(2\pi)^3}\right]\mathrm{dLips}_n(p\to k_1\ldots k_n)\,.\end{aligned}\tag{16}$$

If we would have l photons accompanying n other particles, then the factor in square brackets is iterated. The statistical factor $\frac{1}{l!}$ would complete the form of the phase-space parametrization, similar to the formal expansion of the exponent. The latter formula, supplemented with the definition of the frames with respect to which the angles are defined is used to define the full kinematic configuration of the event. From the angles and energies (k_{γ_i}) of the photons and also of the angles, energies and masses for the other decay products, the four-momenta of all final-state particles can be constructed.

If in (16) instead of $\mathrm{dLips}_n(p\to k_1\ldots k_n)$ one would use $\mathrm{dLips}_n(P\to k_1\ldots k_n)$, then the *tangent space* would be obtained. Then the k_{n+1} photon does not affect the other particles' momenta at all and thus has no boundaries on energy or direction. If this formula would be iterated, then all such photons would be independent from one another as well[6]. Energy and momentum constraints on the photon(s) are introduced with the relation between the tangent and the actual $n+1$-body phase-space. The formula defining one step in the iteration reads as follows[7]:

$$\begin{aligned}&\mathrm{dLips}_{n+1}(P\to k_1\ldots k_n,k_{n+1})=\mathrm{dLips}_n^{+1\,\mathrm{tangent}}\times W_n^{n+1},\\&\mathrm{dLips}_n^{+1\,\mathrm{tangent}}=\mathrm{d}k_\gamma\,\mathrm{d}\cos\theta\,\mathrm{d}\phi\times\mathrm{dLips}_n(P\to\bar{k}_1\ldots\bar{k}_n),\\&\{k_1,\ldots,k_{n+1}\}=\mathbf{T}\big(k_\gamma,\theta,\phi,\{\bar{k}_1,\ldots,\bar{k}_n\}\big).\end{aligned}\tag{17}$$

The W_n^{n+1} depends on details of $\mathbf{T}$ and will thus be given later in (23). To justify (17), we have to convolute (15) for $\mathrm{Lips}_{n+1}(P\to k_1\ldots k_n,k_{n+1})$ with itself (for $\mathrm{Lips}_n(p\to k_1\ldots k_n)$):

$$\begin{aligned}&\mathrm{Lips}_{n+1}(P\to k_1\ldots k_n,k_{n+1})\\&=\frac{\mathrm{d}M_{1\ldots n}^2}{2\pi}\mathrm{Lips}_2(P\to k_{n+1}p)\mathrm{Lips}_n(p\to k_1\ldots k_n),\\&\mathrm{Lips}_n(p\to k_1\ldots k_n)\\&=\frac{\mathrm{d}M_{2\ldots n}^2}{2\pi}\mathrm{Lips}_2(p\to k_1p')\mathrm{Lips}_{n-1}(p'\to k_2\ldots k_n)\end{aligned}\tag{18}$$

and use it also for $\mathrm{Lips}_n(P\to\bar{k}_1\ldots\bar{k}_n)$:

$$\begin{aligned}&\mathrm{Lips}_n(P\to\bar{k}_1\ldots\bar{k}_n)\\&=\frac{\mathrm{d}M_{2\ldots n}^2}{2\pi}\mathrm{Lips}_2(P\to\bar{k}_1\bar{p}')\mathrm{Lips}_{n-1}(\bar{p}'\to\bar{k}_2\ldots\bar{k}_n)\,.\end{aligned}\tag{19}$$

Note that our tangent space of the variables $\mathrm{d}k_\gamma\,\mathrm{d}\cos\theta\,\mathrm{d}\phi$ is unbounded from above, and the limit is introduced by W_n^{n+1}, which is set to zero for the configurations outside the phase-space. In principle, we should distinguish between variables like $M_{2\ldots n}$ for an invariant mass of $k_2\ldots k_n$ and $\bar{M}_{2\ldots n}$ for an invariant mass of $\bar{k}_2\ldots\bar{k}_n$, but in our choice for G_n and G_{n+1} below, $M_{2\ldots n}=\bar{M}_{2\ldots n}$ and $M_{1\ldots n}$ is defined anyway for the $n+1$-body phase-space only.

We refer the reader to [1, 2] for an alternative presentation. Let us remark that (17) is quite general; many options, motivated by the properties of the matrix elements, can be introduced. Generally the transformation T may differ quite a lot from choice to choice. The most straightforward choice can be based on any n- and $n+1$-body phase-space parametrizations using invariant masses and angles (e.g. exactly as in TAUOLA [21] formulas 11 to 13).

If

$$\begin{aligned}G_n:\;&M_{2\ldots n}^2\,,\theta_1\,,\phi_1\,,M_{3\ldots n}^2\,,\theta_2\,,\phi_2\,,\ldots\,,\theta_{n-1}\,,\phi_{n-1}\\&\to\bar{k}_1\ldots\bar{k}_n\end{aligned}\tag{20}$$

and

$$\begin{aligned}G_{n+1}:\;&k_\gamma\,,\theta\,,\phi\,,M_{2\ldots n}^2\,,\theta_1\,,\phi_1\,,M_{3\ldots n}^2\,,\theta_2\,,\phi_2\,,\ldots\,,\\&\theta_{n-1}\,,\phi_{n-1}\\&\to k_1\ldots k_n,k_{n+1}\end{aligned}\tag{21}$$

then

$$\mathbf{T}=G_{n+1}\left(k_\gamma,\theta,\phi,G_n^{-1}\left(\bar{k}_1,\ldots,\bar{k}_n\right)\right).\tag{22}$$

The ratio of the Jacobians (factors $\lambda^{1/2}$ like in (15), etc.) form the factor W_n^{n+1}, which in our case is rather simple,

$$W_n^{n+1}=k_\gamma\frac{1}{2(2\pi)^3}\times\frac{\lambda^{1/2}\left(1,m_1^2/M_{1\ldots n}^2,M_{2\ldots n}^2/M_{1\ldots n}^2\right)}{\lambda^{1/2}\left(1,m_1^2/M^2,M_{2\ldots n}^2/M^2\right)},\tag{23}$$

[5] Let us point out another difference with respect to the angles θ_1^R and ϕ_1^R used in (7) (and also in [16, 21]). For example, if $n=2$, then our $\mathrm{dLips}_{n=2}$ phase-space is parametrized by the angles θ and ϕ only. The two angles will define the orientation of k_γ with respect to the frame used for the quantization of the internal state of k_1, and this is a choice different from the one used for ϕ_1^R, even though $\theta=\theta_1^R$. The Jacobian for the corresponding change of variables equals 1 also.

[6] Expression (16) would be slightly more complicated if instead of photons a massive particle were to be added.

[7] The $\{\bar{k}_1,\ldots,\bar{k}_n\}$ can be identified with the event before the radiation of k_γ is introduced.

because of the choice for G as explained in the appendix. Note that $k_\gamma = \frac{M^2 - M^2_{1\ldots n}}{2M}$. There are additional benefits for such a choice. In all relations $\bar{k}_2 = Lk_2, \ldots, \bar{k}_n = Lk_n$ and $\bar{p}' = Lp'$, a common Lorentz transformation L is used. The transformation L is defined from $k_1, \bar{k}_1, \bar{p}', p'$ and P; the internal relations between the four-vectors $k_2 \ldots k_n$ ($\bar{k}_2 \ldots \bar{k}_n$) are not needed.

Equation (17) can be realized algorithmically in the following way.

1. For any point in n-body phase-space (earlier generated event), described for example with the explicit configuration of four vectors $\bar{k}_1 \ldots \bar{k}_n$, the coordinate variables can be calculated, using (20).
2. Photon variables can be generated according to (17). The weight W_n^{n+1} also has to be attributed.
3. Variables obtained in this way from the old configuration and the one of a photon can be used to construct the new kinematical configuration for the $n+1$-body final state. The phase-space weight, which is zero for configurations outside the phase-space boundaries, can be calculated at this point from (17) and (23) and finally combined with the matrix element.

Here we have chosen two sub-groups of particles. The first one consisted of particle 1 alone, and the second one of particles 2 to n combined. Obviously in the case of two-body decays, as discussed in this paper, there is not much choice when the construction of the first photon is performed.

By iteration, we can generalize (17) to the case of l photons, and we write

$$\begin{aligned}
&\mathrm{dLips}_{n+l}(P \to k_1 \ldots k_n, k_{n+1} \ldots k_{n+l}) \\
&= \frac{1}{l!} \prod_{i=1}^{l} \left[\mathrm{d}k_{\gamma_i}\, \mathrm{d}\cos\theta_{\gamma_i}\, \mathrm{d}\phi_{\gamma_i} W_{n+i-1}^{n+i} \right] \\
&\quad \times \mathrm{dLips}_n(P \to \bar{k}_1 \ldots \bar{k}_n), \\
&\{k_1, \ldots, k_{n+l}\} \\
&= \mathbf{T}\big(k_{\gamma_l}, \theta_{\gamma_l}, \phi_{\gamma_l}, \mathbf{T}\big(\ldots, \mathbf{T}\big(k_{\gamma_1}, \theta_{\gamma_1}, \phi_{\gamma_1}, \\
&\quad \{\bar{k}_1, \ldots, \bar{k}_n\}\big) \ldots\big)\big).
\end{aligned} \tag{24}$$

In this formula we can easily localize the tangent space for the multiple photon configuration. In this space, each photon is independent from the other particles' momenta. Note that it is also possible to fix the upper boundary on k_{γ_i} arbitrarily high. Photons are mutually independent as well. Correlations appear later, thanks to the iterated transformation T. The factors W_{n+i-1}^{n+i} are calculated when the constraints on each consecutive photon are introduced; the previously constructed ones are included in the $n+i-1$ system[8].

Of course, for the tangent space to be useful, the choice of the definition of T must be restricted at least by the condition $\{k_1, \cdots k_n\} \to \{\bar{k}_1, \cdots \bar{k}_n\}$ if all $k_{\gamma_i} \to 0$.[9]

[8] Configurations of k_{γ_i} which cannot be resolved are replaced by the ones with that photon dropped.

[9] In fact, further constraints have to be fulfilled to enable presampling for the collinear singularities.

It is important to realize that one has to choose the matrix elements on the tangent space to complete the construction used in PHOTOS. The number and energies of photons will be generated on the tangent space first. Regularization of (at least) a soft singularity must be defined. Rejection and event construction are performed with the help of (17) for each consecutive photon. It diminishes the photon multiplicity with respect to the one defined for the tangent space. Of course, as a rejection implements changes in the phase-space density, a matrix element (with virtual corrections) of the physical space can be introduced as well.

The treatment of the phase-space presented here lies at the heart of the construction of PHOTOS kinematics and has been used since its beginning. It exhausts the case when there is only one charged particle in the final state. For multiple charged particle final states a new complication appears, because all collinear configurations need simultaneous attention, and not only the one along the k_1 direction. A presampler with multichannel generation is needed. In our case we follow the same method[10] as explained in [21].

In the standard version of PHOTOS, as published in [1, 2], the following matrix element is used for single photon emission when there is *only one charged particle* in the final state:

$$|\mathcal{M}|^2_{\mathrm{PHOTOS}} = |A^{\mathrm{Born}}|^2 \mathrm{WT}_3^{\mathrm{old}}\,, \tag{25}$$

where

$$\begin{aligned}
\mathrm{WT}_3^{\mathrm{old}} &= \frac{4\pi\alpha}{\mathrm{WT}_1 \mathrm{WT}_2} \frac{2(1-x)}{1+(1-x)^2} \left(1 - \frac{m_R^2}{1-\beta^2\cos^2\theta}\right) \\
&\quad \times \frac{1+\beta\cos\theta}{2} \frac{1-\sqrt{1-m_R^2}\cos\theta}{1-\beta\cos\theta}\,, \\
\beta &= \sqrt{1 - 4\frac{m_1^2}{M^2(1-x)} \frac{1}{(1-x+(m_1^2-m_2^2)/M^2)^2}}\,, \\
x &= \frac{2E_\gamma}{M} \frac{M^2}{M^2-(m_1+m_2)^2}\,, \\
m_R^2 &= 4\frac{m_1^2}{M^2(1+m_1^2/M^2)^2}\,.
\end{aligned} \tag{26}$$

The old and lengthy approximation $\mathrm{WT}_3^{\mathrm{old}}$ for WT_3 implemented in standard PHOTOS is kept for compatibility with [2]. The expression defining WT_3 without approximations reads

$$\begin{aligned}
|\mathcal{M}|^2_{\mathrm{exact}} &= |A^{\mathrm{Born}}|^2 4\pi\alpha \left(q_1 \frac{k_1.\epsilon}{k_1.k_\gamma} - q\frac{P.\epsilon}{P.k_\gamma}\right)^2 \\
&= |A^{\mathrm{Born}}|^2 4\pi\alpha \frac{8}{M^2} \times \mathrm{WT}_3(P, k_1, k_2, k_\gamma)\,,
\end{aligned}$$

Note that the variables $k_{\gamma_m}, \theta_{\gamma_m}, \phi_{\gamma_m}$ are used at the time of the mth step of the iteration only, and they are not needed elsewhere in the construction of the physical phase-space; the same is true for the invariants and angles $M^2_{2\ldots n}, \theta_1, \phi_1, \ldots, \theta_{n-1}, \phi_{n-1} \to \bar{k}_1 \ldots \bar{k}_n$ of (20) and (21), which are also redefined at each step of the iteration.

[10] We will omit details here, because for the two-body final states the complications manifest themselves only in the case of multiple photon generation; see the appendix.

$$
\begin{aligned}
&''\mathrm{WT}_3(P,k_1,k_2,k_\gamma)\\
&=\frac{\left(\frac{M}{2E_\gamma}\right)^2\lambda\left(1,\frac{m_1^2}{\tau},\frac{m_2^2}{\tau}\right)\left(1-\frac{2E_\gamma}{M}\right)\sin^2\theta}{2\Big(1+\frac{m_1^2-m_2^2}{\tau}-\lambda^{1/2}\left(1,\frac{m_1^2}{\tau},\frac{m_2^2}{\tau}\right)\cos\theta\Big)^2}\,; \qquad (27)
\end{aligned}
$$

here, $\tau=(k_1+k_2)^2$. In both the standard and exact version of PHOTOS, the same phase-space parametrization and presampler for collinear and soft singularities are used. Together with WT_3 the following WT_1 and WT_2 factors related to the phase-space contribute to the final weight implemented in the routine PHOCOR of PHOTOS:

$$
\begin{aligned}
\mathrm{WT}_1(P,k_1,k_2,k_\gamma)&=\frac{\lambda^{1/2}\left(1,\frac{m_1^2}{M^2},\frac{m_2^2}{M^2}\right)}{\lambda^{1/2}\left(1,\frac{m_1^2}{\tau},\frac{m_2^2}{\tau}\right)}\frac{2E_\gamma}{M}\,,\\
\mathrm{WT}_2(P,k_1,k_2,k_\gamma)&=\frac{2(1-\cos\theta\sqrt{1-m_R^2})}{1+(1-x)^2}\frac{M}{2E_\gamma}\,.
\end{aligned}
\qquad (28)
$$

The expression for WT_1 can be deciphered from (17), and WT_2 is related to the presamplers for the collinear and soft singularities. The factors WT_1 and WT_2 are only used in the present paper in the definition of $\mathrm{WT}_3^{\mathrm{old}}$; see (26).

The combined effect of the virtual and real corrections on the total rate is manifest through $\frac{\Gamma^{\mathrm{Total}}}{\Gamma^{\mathrm{Born}}}$. The virtual corrections are included into PHOTOS through this factor. Let us point out that the ratio of (27) and (25) constitutes the basic element of upgrading the PHOTOS functionality to the complete first order[11]. The correcting weight can be chosen simply as

$$
\mathrm{wt}=\frac{|\mathcal{M}|^2_{\mathrm{exact}}}{|\mathcal{M}|^2_{\mathrm{PHOTOS}}}\frac{\Gamma^{\mathrm{Born}}}{\Gamma^{\mathrm{Total}}}\,. \qquad (29)
$$

For the standard version of PHOTOS the virtual corrections are required to be such that the total decay rate remains unchanged after complete QED corrections are included.

In the case of final states with two charged particles in PHOTOS, (29) needs to be modified with one of the following versions of the interference weight:

$$
\begin{aligned}
\mathrm{wt}&=\sum_{i=1,2}\frac{|\mathcal{M}|^2_{\mathrm{exact}}}{|\mathcal{M}|^2_{\mathrm{PHOTOS}}}\bigg|_i\frac{\Gamma^{\mathrm{Born}}}{\Gamma^{\mathrm{Total}}}\mathrm{WT}^i_{\mathrm{INT}}\,,\\
\mathrm{WT}^i_{\mathrm{INT}}&=\frac{\left(q_1\frac{k_1.\epsilon}{k_1.k_\gamma}-q_2\frac{k_2.\epsilon}{k_2.k_\gamma}\right)^2}{\left(q_1\frac{k_1.\epsilon}{k_1.k_\gamma}-q_1\frac{P.\epsilon}{P.k_\gamma}\right)^2+\left(q_2\frac{k_2.\epsilon}{k_2.k_\gamma}-q_2\frac{P.\epsilon}{P.k_\gamma}\right)^2}\,,
\end{aligned}
$$

$$
\begin{aligned}
\mathrm{WT}^i_{\mathrm{INT-opt.}}&=J_i\left(q_1\frac{k_1.\epsilon}{k_1.k_\gamma}-q_2\frac{k_2.\epsilon}{k_2.k_\gamma}\right)^2\\
&\quad\Bigg/\left(\left(q_1\frac{k_1.\epsilon}{k_1.k_\gamma}-q_1\frac{P.\epsilon}{P.k_\gamma}\right)^2J_1\right.\\
&\quad\left.+\left(q_2\frac{k_2.\epsilon}{k_2.k_\gamma}-q_2\frac{P.\epsilon}{P.k_\gamma}\right)^2J_2\right)\,,\\
J_1&=\frac{1}{\mathrm{WT}_1(P,k_1,k_2,k_\gamma)\mathrm{WT}_2(P,k_1,k_2,k_\gamma)}\,,\\
J_2&=\frac{1}{\mathrm{WT}_1(P,k_2,k_1,k_\gamma)\mathrm{WT}_2(P,k_2,k_1,k_\gamma)}\,.
\end{aligned}
\qquad (30)
$$

The sum over two generation channels $i=1,2$ related to the emission from q_1 and q_2 is to be performed[12]. The form of $\mathrm{WT}^i_{\mathrm{INT}}$ results from the exact expressions, (12) and (6). However, the phase-space and multichannel presampler specific terms (28) need to be discussed. The presence of J_1 and J_2 in the interference weight is optional, but only for single photon radiation. The factor $J_{1,2}$ (J_1 or J_2) should cancel the $\mathrm{WT}_1\cdot\mathrm{WT}_2$ term of the generation branch used for this particular event generation. In general, the absence of $J_{1,2}$ terms is due to the properties of the second order matrix element[13]. For the time being, analogs to the case of Z decay have to be used instead of the proof.

Once we have completed the description of our internal correcting weight necessary for PHOTOS to work in the NLO regime, we will turn to the numerical results.

4 Results of the tests

The most attractive property of Monte Carlo is the possibility to implement selection criteria for the theoretical predictions that coincide with the experimental ones. Especially in the case of the final state bremsstrahlung the presence of experimental cut-offs is essential, as they usually significantly increase the size of the QED effects.

In this section we will concentrate, however, on the following pseudo-observables, as used in [22, 23].

- The photon energy in the decaying particle rest frame: this observable is sensitive mainly to the leading-log (i.e. collinear) non-infrared (i.e. not soft) component of the distributions.
- The energy of the final-state charged particle: as the previous one, this observable is sensitive mainly to the leading-log (i.e. collinear) non-infrared (i.e. not soft) component of the distributions.

[11] When the option of multiple radiation is used in PHOTOS, the single photon emission kernel is iterated. This leads to some complications.

[12] Equations (27) and (25) for $|\mathcal{M}|^2_{\mathrm{exact}}$ and $|\mathcal{M}|^2_{\mathrm{PHOTOS}}$ are for the emissions in case of a single charge final state only; the interference weight is to introduce the exact matrix element for a process with two charged scalar final state.

[13] For example, the form $\mathrm{WT}_{INT-option}$ is inappropriate for configurations in which the first generated photon is hard and the second one soft.

– The angle of the photon with final-state charged particle: this observable is sensitive mainly to the non-collinear (i.e. non-leading-log) but soft (i.e. infrared) component of the distributions.
– The acollinearity angle of the final-state scalars: this observable is sensitive mainly to the non-collinear (i.e. non-leading-log) and non-soft (i.e. non-infrared) component of the distributions.

We will start our comparison for $B^- \to \pi^0 K^-(\gamma)$ and PHOTOS running without improvements from the complete matrix element: the agreement looks good, see Fig. 1, and holds over the entire range of distributions, even though the densities vary by up to 8 orders of magnitude. Differences can hardly be seen. To visualize the differences, in Fig. 2, the ratios of the distributions are plotted. Similar to what was seen in the tests for Z decays [14] local discrepancies may reach up to 15% for $\cos\theta_{\text{acoll.}} > 0.5$. Note however that those regions of the phase-space contribute at the level of 10^{-6} to the total decay rate. Once the matrix element is switched on, see Fig. 3, where the ratios of the distribution are plotted, the agreement becomes excellent, even at a statistical level of 10^9 events. It was of no use to repeat the plots of the distributions with the corrected weight in PHOTOS, as the plots could not be distinguished from the ones of Fig. 1.

Encouraged by the excellent performance in the case of the decay into final states with a single charged particle, let us now turn to decays into two charged mesons. To avoid accidental simplifications, we have selected final states with scalars of different masses ($B^0 \to \pi^- K^+(\gamma)$).

Again, as can be seen from Figs. 4 and 5, agreement between PHOTOS using the standard kernel and SANC is rather good, but some differences persist. Once the complete kernel is switched on, see Fig. 6, the agreement is quite amazing. In this case, the interference weight and the multiple singularity structure of the presampler Jacobians, see (30), were tested as well. Both versions, WT_{INT} and $\text{WT}_{\text{INT-option}}$, gave the same results for the case of single photon emission. However, only the first version, WT_{INT}, turned out to be consistent with exponentiation. To complete the tests for multichannel emissions, final states with more than two massive decay products need to be studied, preferably for multiphoton radiation as well.

Let us comment that not only the shapes of the distribution agree in an excellent manner for the PHOTOS and SANC simulations; also the number of events with photons of energy below a certain threshold agreed better than 0.01%, and they thus were consistent with each other within a statistical error of 10^9 event samples. The excellent agreement presented in our paper combined with other results published before help to confirm that theoretical effects normally missing in PHOTOS are small, but if

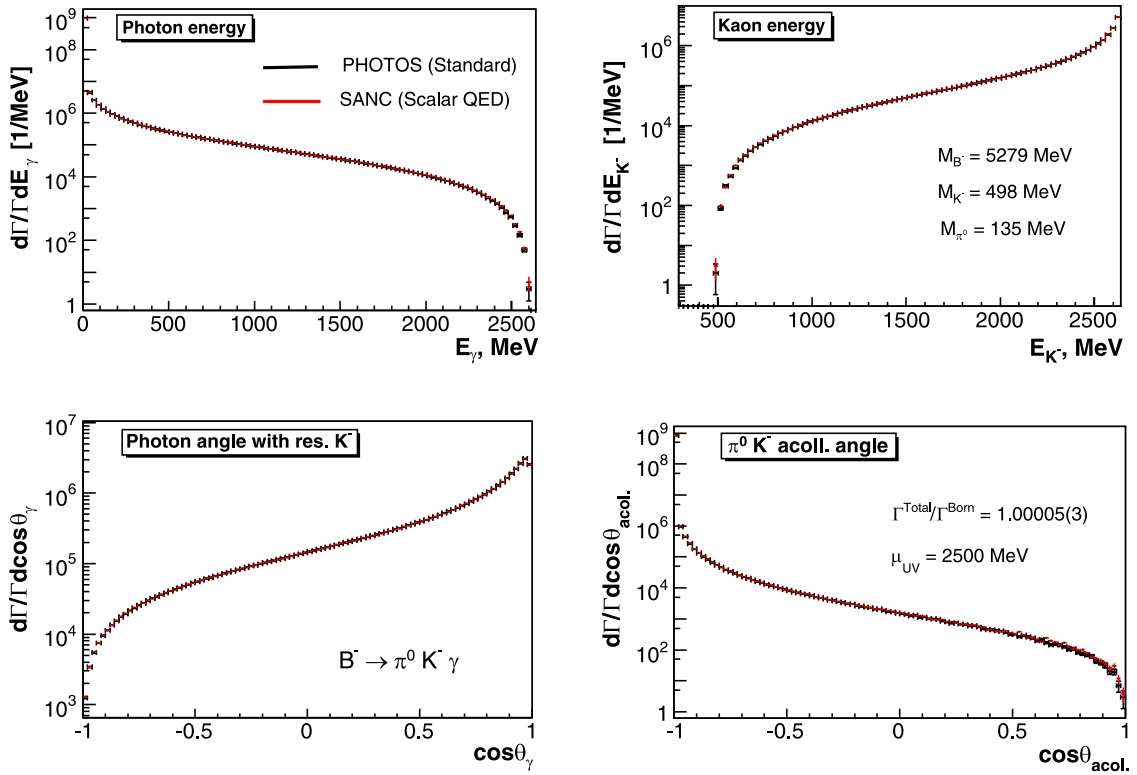

Fig. 1. Results from PHOTOS, standard version, and SANC for $B^- \to \pi^0 K^-(\gamma)$ decay are superimposed on the consecutive plots. Standard distributions, as defined in the text, and logarithmic scales are used. The distributions from the two programs overlap almost completely. Samples of 10^9 events were used. The ultraviolet scale, μ_{UV}, was chosen to leave the total decay width unchanged by QED

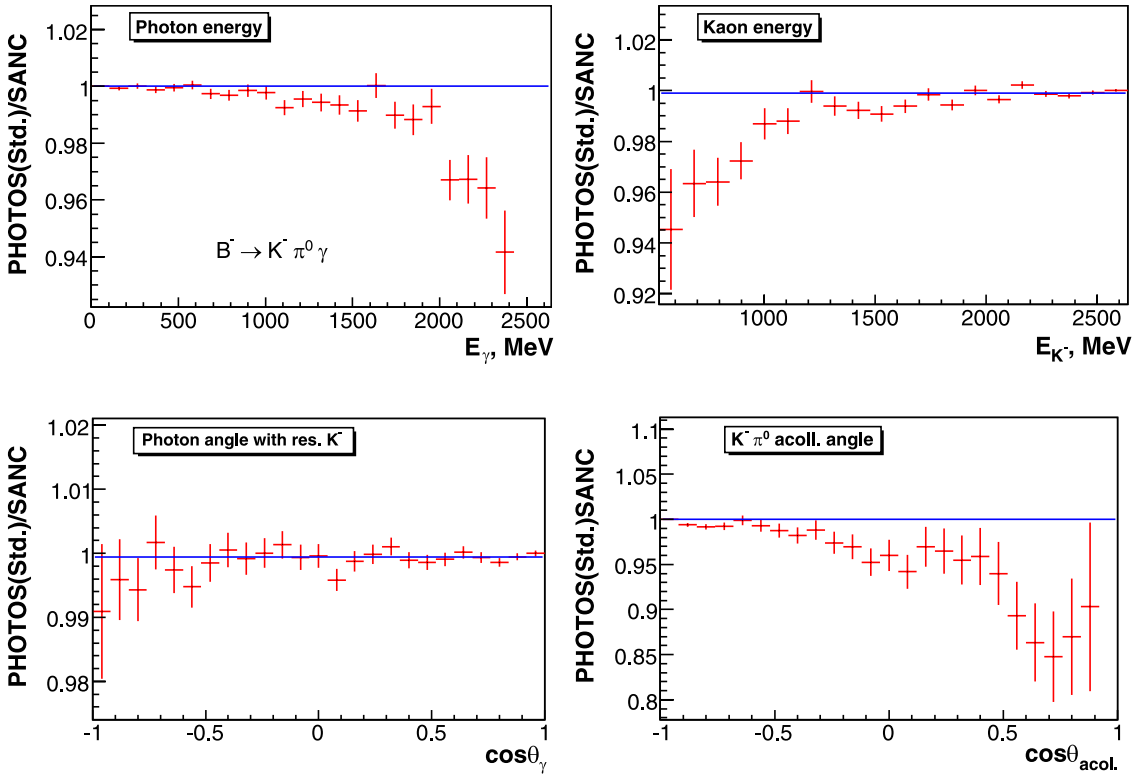

Fig. 2. Results from PHOTOS, standard version, and SANC for the ratios of the $B^- \to \pi^0 K^-(\gamma)$ distribution in Fig. 1 are presented. Differences between PHOTOS and SANC are small, but are clearly visible now

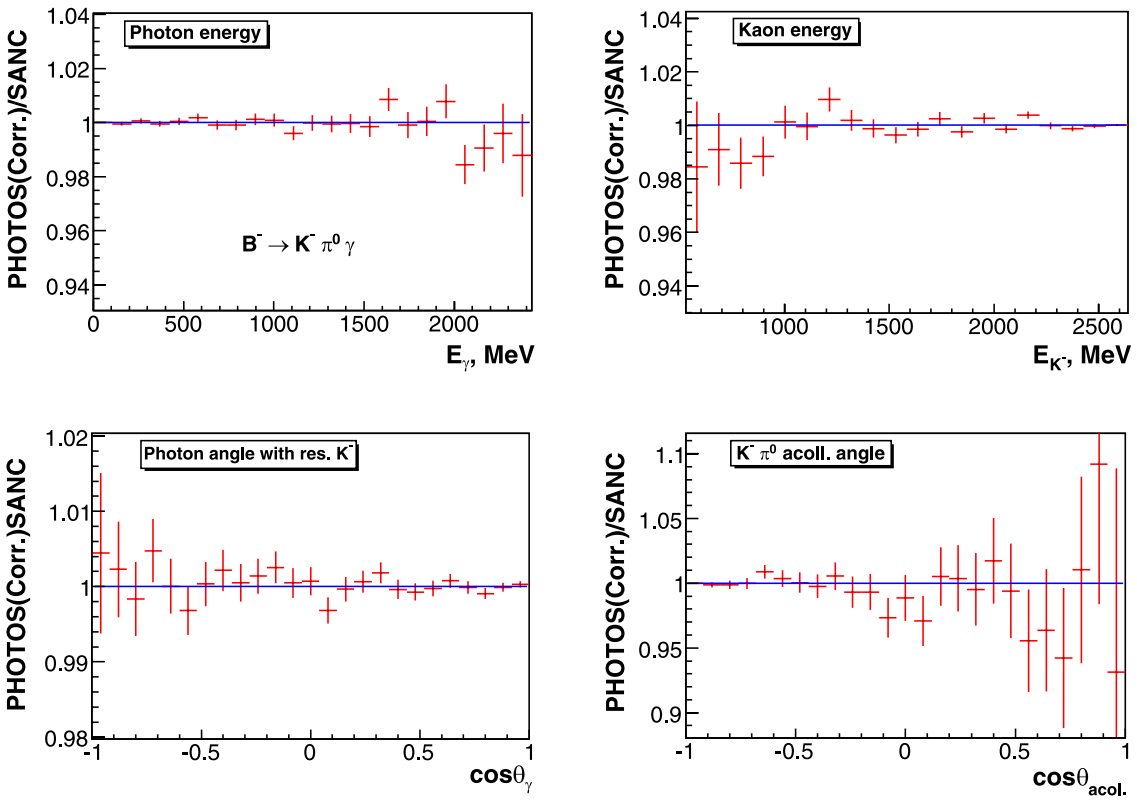

Fig. 3. Results from PHOTOS with the exact matrix element, and SANC for ratios of the $B^- \to \pi^0 K^-(\gamma)$ distributions. Differences between PHOTOS and SANC are below statistical error for samples of 10^9 events

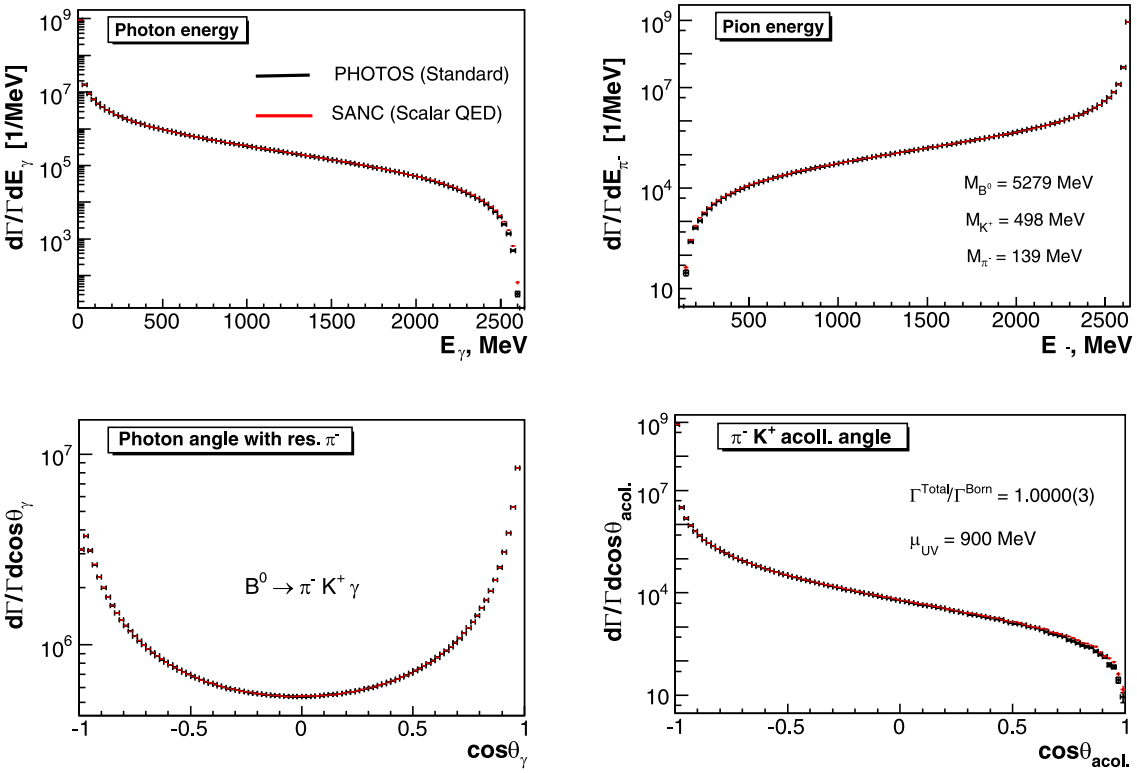

Fig. 4. Results from PHOTOS, standard version, and SANC for $B^0 \to \pi^- K^+(\gamma)$ decay are superimposed on the consecutive plots. Standard distributions, as defined in the text, and logarithmic scales are used. The distributions from the two programs overlap almost completely. Samples of 10^9 events were used. The ultraviolet scale, $\mu_{\rm UV}$, was chosen to leave the total decay width unchanged by QED

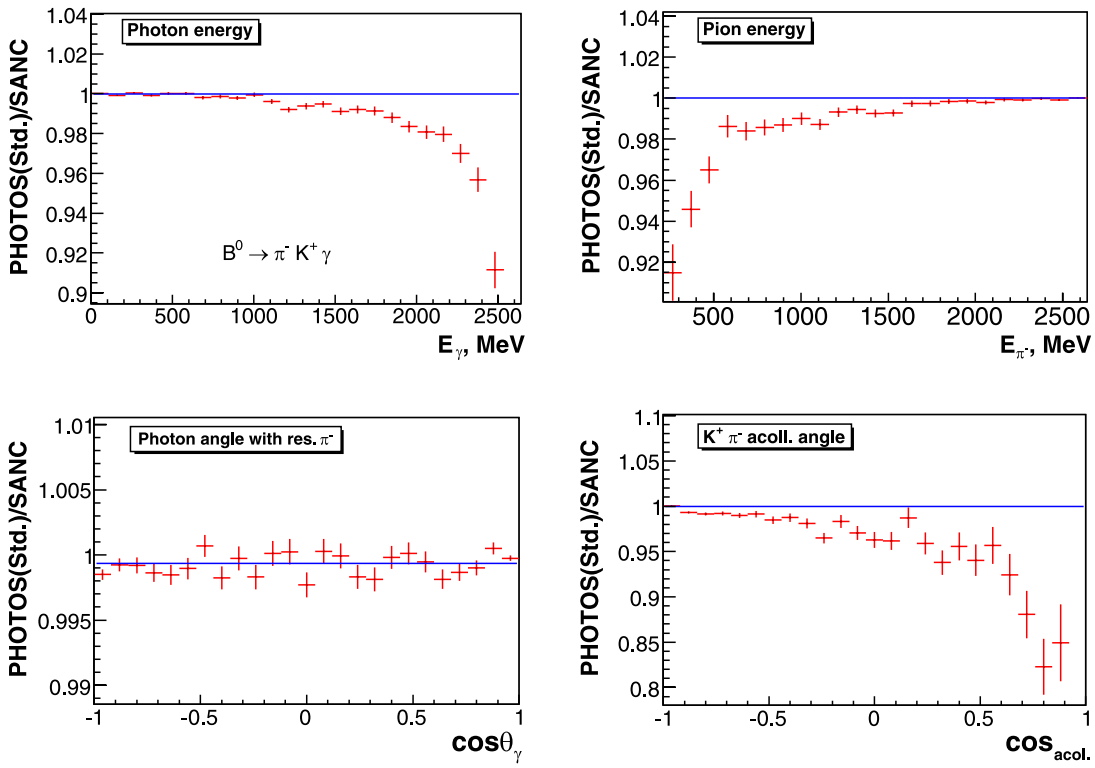

Fig. 5. Results from PHOTOS, standard version, and SANC for the ratios of the $B^0 \to \pi^- K^+(\gamma)$ distributions in Fig. 4 are presented. Differences between PHOTOS and SANC are small, but are clearly visible now

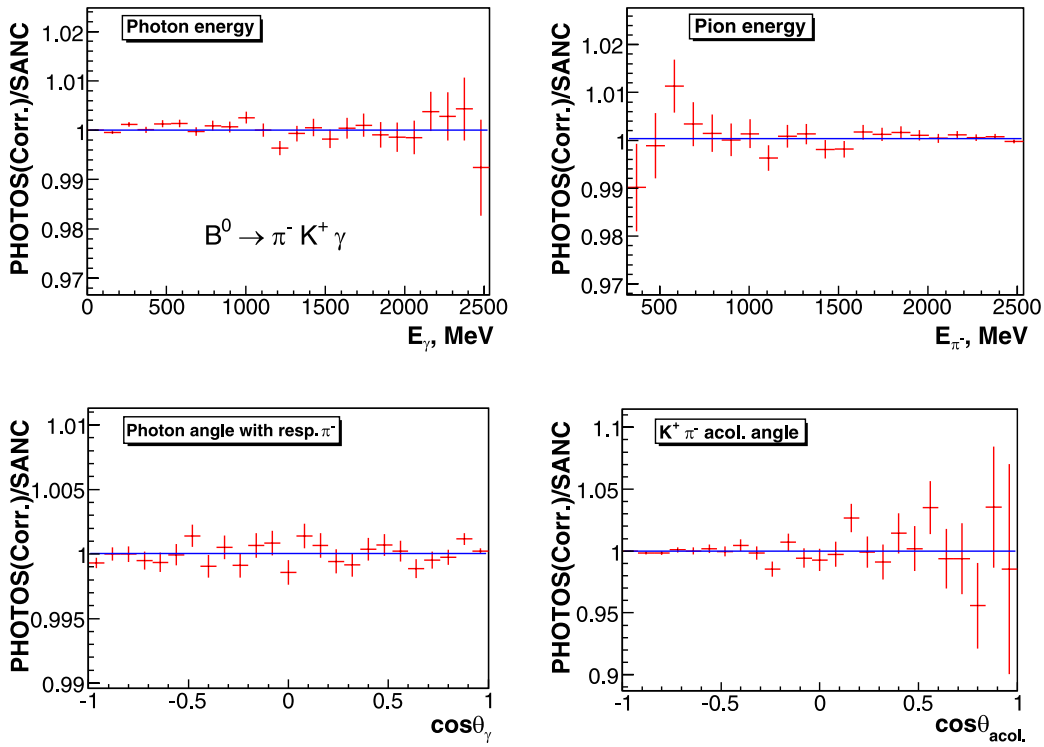

Fig. 6. Results from PHOTOS with the exact matrix element, and SANC for the ratios of the $B^0 \to \pi^- K^+(\gamma)$ distributions. Differences between PHOTOS and SANC are below statistical error for samples of 10^9 events

Table 2. Benchmark results for B decays into pair of scalars: electromagnetic cumulative of decay width $\Gamma(E_{\rm test})/\Gamma^{\rm Total}$, where $E_{\rm test}$ denotes the maximal energy which can be carried out by photons. The following input parameters were used: $m_B = 5279$ MeV, $m_{\pi^0} = 135$ MeV, $m_{\pi^\pm} = 139$ MeV, $m_{K^0} = 494$ MeV, $m_{K^\pm} = 498$ MeV. For the B^- decays $\mu_{\rm UV} = 2500$ MeV, while for the B^0 decays $\mu_{\rm UV} = 900$ MeV. Our results differ negligibly between standard PHOTOS and the one with exact matrix element; that is why only one set of numerical results is provided. For each decay channel PHOTOS results of first, second and multiple photon radiation are to a good precision in the following proportion $1-x : 1-x+x^2/2 : \exp(-x)$, where x for each line of the table is different; it depends on the decay channel and $E_{\rm test}$. To produce the results for our table, samples of 10^7 events were used. Statistical errors are thus at the level of the last significant digit for all the table entries

Channel	$E_{\rm test}$ MeV	SANC	PHOTOS $\mathcal{O}(\alpha)$	$\mathcal{O}(\alpha^2)$	$\mathcal{O}(exp)$
$B^- \to \pi^-\pi^0$	2.6	0.9291	0.9289	0.9314	0.9311
$B^- \to \pi^-\pi^0$	26	0.9571	0.9569	0.9578	0.9577
$B^- \to \pi^- K^0$	2.6	0.9294	0.9292	0.9318	0.9314
$B^- \to \pi^- K^0$	26	0.9574	0.9572	0.9580	0.9580
$B^- \to K^-\pi^0$	2.6	0.9627	0.9628	0.9636	0.9634
$B^- \to K^-\pi^0$	26	0.9777	0.9777	0.9779	0.9779
$B^- \to K^- K^0$	2.6	0.9629	0.9631	0.9639	0.9638
$B^- \to K^- K^0$	26	0.9779	0.9779	0.9782	0.9781
$B^0 \to \pi^-\pi^+$	2.6	0.8311	0.8306	0.8451	0.8433
$B^0 \to \pi^-\pi^+$	26	0.8978	0.8972	0.9019	0.9016
$B^0 \to \pi^- K^+$	2.6	0.8662	0.8660	0.8754	0.8741
$B^0 \to \pi^- K^+$	26	0.9193	0.9188	0.9219	0.9219
$B^0 \to K^-\pi^+$	2.6	0.8661	0.8659	0.8753	0.8743
$B^0 \to K^-\pi^+$	26	0.9193	0.9191	0.9220	0.9219
$B^0 \to K^- K^+$	2.6	0.9011	0.9014	0.9066	0.9057
$B^0 \to K^- K^+$	26	0.9407	0.9407	0.9424	0.9422

necessary these can be introduced into the code. It is also important to note that the agreement provides a powerful technical test of the generator.

Finally, let us point out that early versions of the program, before 2004, were not reaching that level of technical sophistication. To establish it required a major effort. Kinematical variables used in PHOTOS differ from those of SANC. The differences could arise due to technical problems, but also if for example the Born level events that are to be modified by PHOTOS would not fulfill energy-momentum conservation, or if the particles' momenta were not on mass-shell, at the numerical double precision level. This point must always be checked for every new installation of PHOTOS in an experimental environment. For that purpose we have collected numerical results, given in Table 2 for the cumulant of the bremsstrahlung decay width $G(E_{\rm test}) = \Gamma(E_{\rm test})/\Gamma^{\rm Total}$, where $\Gamma(E_{\rm test})$ denotes the decay width integrated over the energy carried by all bremsstrahlung photons combined up to maximum of $E_{\rm test}$.

5 Summary

This paper was devoted to the study of bremsstrahlung corrections in the decay of B mesons into pair of scalars of rather large masses. The results were presented in analytical form and in the form of Monte Carlo simulations, which were later compared.

To quantify the size of the next to leading order effects normally missing in PHOTOS, we have installed into the program the complete scalar QED first order expression for the B decay matrix element. After modification, the differences between PHOTOS and the matrix element calculation embodied in SANC were below statistical error of 10^9 events for all of our benchmark distributions. Both PHOTOS and SANC were run at fixed first order without exponentiation. The agreement provides a technical test of the simulations from the two programs as well.

The improvement of the agreement due to the introduction of a correcting weight could come but at a price. That was the case with the decay of Z. However, because our B mesons are scalar, the complications did not materialize and a correcting weight can be installed to the standard PHOTOS versions. On the other hand, the improvements introduced are numerically small. The deficiencies of standard PHOTOS are localized in the corners of bremsstrahlung phase-space populated by photons of very high energies and angularly well separated from the final state mesons. Those regions of the phase space weigh less than 0.005 of the total rate, and differences in that region approach 20% of their size, at most. The effects are thus significantly lower than 0.1%, if quantified in units of the integrated B decay rate of a particular channel. Also, in those regions, the predictive power of scalar QED is rather doubtful. That is why we do not think it is urgent for users to change the PHOTOS correcting weight to enable the complete NLO, unless the measured form-factors become available. The contribution to the systematic error of PHOTOS due to incompleteness of the old kernel (with respect to scalar QED) does not depend on experimental cuts and is thus of no phenomenological importance for today.

Our paper was not only focused on numerical results due to final-state bremsstrahlung in B decays. Aspects of the mathematical organization of the program for the calculation of radiative corrections for B production and decay have been discussed as well. The approximations used in PHOTOS affect the matrix elements and *not* the phase-space, which is treated exactly including all mass effects.

Details of phase-space parametrization and other aspects necessary for the implementation of the NLO effects are collected for the first time. Generation of the phase-space starts from the tangent space constructed from an eikonal approximation but used also for the hard photons, even of energies above the available maximum. In the second step, phase-space constraints are enforced. The method is similar to exclusive exponentiation [24].

A complete re-analysis of the final weight for decays into scalars was presented. Parts corresponding to the matrix elements, phase-space Jacobians and generator presamples were explicitly separated. Special care was given to the mass terms. The analytic form of the single photon emission kernel (i.e. the matrix element with approximation) used in the standard version of PHOTOS was also explicitly given. That is why the analysis presented here can easily be extended to other decay channels. It is the first time that we have presented such a study for particles other than elementary fermions and in the case in which mass terms of order $\frac{\alpha}{\pi}\frac{m_{1,2}^2}{M^2}$ are not neglected. Our analytical calculations exactly agree with the results of [19] and could serve as a basis of our technical tests of the program.

The numerical results collected in Table 2 can be used as a technical test of the PHOTOS installation in end-user simulation set-ups. We strongly recommend such tests to be performed. In these tests the agreement between PHOTOS and SANC (or simple semi-analytical expressions for higher order simulations) was significantly better than 0.1% for all entries.

In the case that the program operates for multiple photon radiation, energy momentum constraints are introduced for each consecutive photon, step by step, and conformal symmetry is not exploited in that procedure. Details of the phase-space parametrization used for multiple photon radiation were presented. In principle, for B decays and multiple photon radiation in PHOTOS, a similar level of agreement as in [14] for Z decay is expected, but the appropriate reference distributions do not exist yet. In particular, the second order scalar QED matrix element for B decays was not available for us. That is why we think that the matrix-element related details of the program construction, necessary for the implementation of NLL effects in the general case, must remain delegated to forthcoming work; probably to the times that we will have at our disposal other second order matrix elements than just those of $Z \to l\bar{l}$. At present, only the dispersed results (and for NLL based on analogies with Z decays only) of [2, 14, 25] are available for that purpose.

PHOTOS used for the decays of B mesons into scalars provides an example of a program working for multiple emissions from both outgoing charged lines. It covers complete phase-space, and no special treatment is needed for the hard photon emission regions. Also mass terms have been included without any approximations.

On the technical level it is worth mentioning that the NLO correcting weight of PHOTOS is used as an internal weight. All generated events remain of weight 1, exactly as it was in the case of $Z \to \mu^+\mu^-$ decay.

In principle, if necessary, even complete higher order matrix elements (NNLO level) could be incorporated with the help of correcting weights. This interesting point definitely goes beyond the scope of the present paper and also beyond phenomenological interest for any foreseeable future. This is equally true for the possible extensions to simulations in QCD, which are also outside the scope of the paper.

Acknowledgements. Useful discussions with E. Barberio, P. Golonka, Z. Nagy, F. Tkachov and T. Sjöstrand are acknowledged.

Appendix: Details and properties of the explicit phase-space parametrization

Equations (17) and (24) are central in the definition of the PHOTOS algorithm and its phase-space parametrization. For the general description details were not important. In practice, they are nonetheless essential, and all angles and masses (or energies) used in (20) and (21) must be specified. In particular, all reference frames used in the definition of the angles must be defined.

We will start with the detailed description of the parametrizations for two-body and three-body phase-spaces; the latter one with an additional single photon, which accompanies the final state of two massive objects (not necessarily of equal masses). In both cases, the decay of an object of mass M and four-momentum P is taken into account. The straightforward extension for the parametrization of the multibody decay will be introduced with the help of the footnote; properties will be discussed later in the text.

Our particular choice of the phase-space parametrization is of course motivated by the necessity to regularize the infrared and collinear singularities. On the other hand, the definition itself does not need singularities to be exposed, or even to be present at all. For easy reading, let us point out that (at first) we will expect the collinear singularity to be present only when the photon becomes parallel to the direction of k_1. Later, we will discuss the case when both final states (of momentum k_1 and k_2) are charged and thus the singularity may appear along the two directions. We will continue with the case when the photon accompanies a multiparticle/multicharge final state and with the necessity to introduce several simultaneous parametrizations, to be used in Monte Carlo parallel generation *channels*, used at each step of iteration as defined in (24).

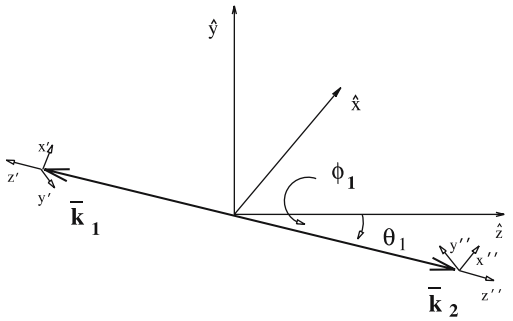

Fig. 7. The angles θ_1, ϕ_1 defined in the rest–frame of P and used in parametrization of two-body phase-space

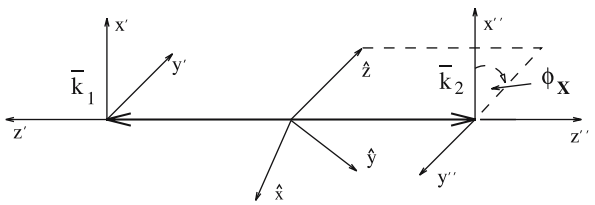

Fig. 8. The angle ϕ_X is also defined in the rest frame of P as the angle between (oriented) planes spanned on: (i) $\bar{k}_1$ and $\hat{z}$ axis of the P rest frame system, and (ii) $\bar{k}_1$ and x'' axis of the $\bar{k}_2$ rest frame. It completes the definition of the phase-space variables if the internal orientation of $\bar{k}_1$ system is of interest. In fact, the Euler angle ϕ_X is inherited from unspecified details, the parametrization of phase-space used to describe possible future decay of $\bar{k}_2$ (or $\bar{k}_1$)

In the following eight points we define the angles used for the two-body phase-space parametrization, and we continue with the definition of the phase-space variables of the two-body plus photon case.

1. For the definition of the coordinate system in the P rest frame the $\hat{x}$ and $\hat{y}$ axes of the laboratory frame boosted to the rest frame of P can be used. The orthogonal right-handed system can be constructed with their help in a standard way.
2. We choose polar angles θ_1 and ϕ_1 defining the orientation of the four-momentum $\bar{k}_2$ in the rest frame of P. In that frame $\bar{k}_1$ and $\bar{k}_2$ are back to back[14]; see Fig. 7.
3. The previous two points would complete the definition of the two-body phase-space, if both $\bar{k}_1$ and $\bar{k}_2$ had no measurable spin degrees of freedom visualizing themselves e.g. through correlations of the secondary decay products' momenta. Otherwise we need to know an additional angle ϕ_X to complete the set of Euler angles defining the relative orientation of the axes of the P rest frame system with the coordinate system used in the rest frame of $\bar{k}_2$ (and possibly also of $\bar{k}_1$); see Fig. 8.

[14] In the case of a phase-space construction for multibody decays $\bar{k}_2$ should be read as a state representing the sum of all decay products of P but $\bar{k}_1$.

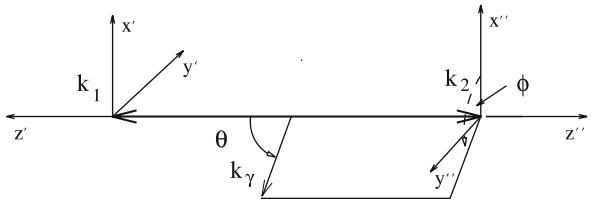

Fig. 9. The angles θ, ϕ are used to construct the four-momentum of k_γ in the rest frame of k_1+k_2 pair (itself not yet oriented with respect to P rest frame). To calculate the energies of k_1, k_2 and the photon, it is enough to know m_1, m_2, M and the photon energy k_γ of the P rest frame

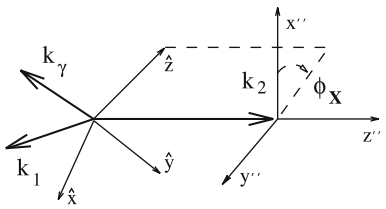

Fig. 10. Use of angle ϕ_x in defining the orientation of k_1, k_2 and the photon in the rest frame of P. At this step only the plane spanned on the P frame axis $\hat{z}$ and k_2 is oriented with respect to the $k_2 \times x''$ plane

4. If both the rest frames of $\bar{k}_1$ and $\bar{k}_2$ are of interest, their coordinate systems are oriented with respect to P with the help of θ_1, ϕ_1 and ϕ_X. We assume that the coordinate systems of $\bar{k}_1$ and $\bar{k}_2$ are connected by a boost along the $\bar{k}_2$ direction, and in fact share axes: $z' \uparrow\downarrow z''$, $x' \uparrow\uparrow x''$ and $y' \uparrow\downarrow y''$.
5. Let us turn now to the three-body phase-space parametrization. We take the photon energy k_γ in the rest frame of P, and with its help we calculate the photon energies, k_1 and k_2, all in the k_1+k_2 frame.
6. We use the angles θ and ϕ in the rest frame of the k_1+k_2 pair: θ is the angle between the photon and the direction of k_1 (i.e. $-z''$). The angle ϕ defines the photon azimuthal angle around z'' with respect to the x'' axis (of the k_2 rest frame); see Fig. 9.
7. If all k_1, k_2 and k_1+k_2 rest frames exist, then the x axes for the three frames are chosen to coincide. This is possible, because they are all connected by the boosts along the common z'' direction; see Fig. 9. The axes of the k_1+k_2 rest frame are not drawn explicitly.
8. To define the orientation of k_2 in the P rest frame coordinate system, and to complete the construction of the whole event, we will re-use the Euler angles of $\bar{k}_2$: ϕ_X, θ_1 and ϕ_1 (see Figs. 10 and 11), defined again, of course, in the rest frame of P.

This completes our definitions of the parametrizations for the two-body and three-body phase-spaces necessary to define the transformation G of (20) and (21). Before commenting on the properties of our parametrizations, let us note that these parametrizations were already used and defined in [2], in full detail, except for the function of the angle ϕ_X (only implicitly introduced there). For some readers, the definition from that paper may also be easier to follow.

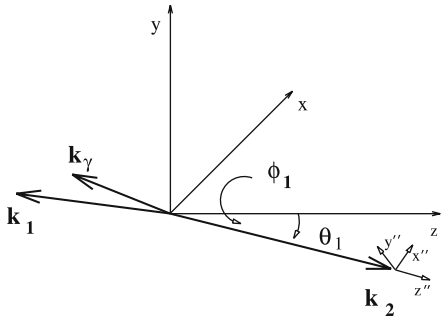

Fig. 11. Final step in the event construction. The angles θ_1 and ϕ_1 are used. The final orientation of k_2 coincides with this of $\bar{k}_2$

Let us comment, now, on those properties of our parametrizations that are important for the construction of the PHOTOS algorithm.

a) The parametrizations of the two-body and three-body phase-space (photon included) are used for the explicit kinematical construction denoted by (17). We can exchange the roles played by k_1 and k_2. This simple operation leads to a new phase-space parametrization, which can be used in a second branch of the Monte Carlo generation.
b) The phase-space Jacobians (factor W_n^{n+1} of (17)) are identical for the two branches; this factor is also never larger than $k_\gamma \frac{1}{2(2\pi)^3}$.
c) The angle θ of the first branch coincides with $\pi-\theta$ of the second one.
d) In the soft ($k_\gamma \to 0$) and collinear ($\theta \to 0$ or π) limits, the angles θ_1, ϕ_1 and ϕ_X of the two branches converge to each other (in these limits they may differ by π or 2π).
e) Properties c) and d) are convenient for our construction of the weights given by (30), because they coincide with the similar properties of the exact matrix element.
f) Thanks to property b), also the first version of (30) is exact. In fact, this first version is more suitable for multiphoton radiation, if the first order matrix element is used only. This observation required comparisons with second order matrix elements [14]. The choice of the $\bar{k}_2$ (or k_2) direction to define θ_1 and ϕ_1, rather than $\bar{k}_1$, was also motivated by the properties of the decay matrix elements.

Let us now present some further observations[15], which go beyond NLO corrections for the processes discussed in [14] and in the present paper and point out applications for multibody/multicharge final states.

– Property d) extends to more than two-body decays and also to cases in which there are more than two charged

[15] Note that the approximations to be discussed in the following points result from matching kinematical branches and affect the way how phase-space Jacobians are used in (30). The full phase-space remains covered, as is the case of (17) and (24) denoting exact phase-space parametrization of single and multiphoton final states.

particles present in the final state. The relation between the angles θ_1, ϕ_1 and ϕ_X of the distinct branches is more complex, but it is in the limits discussed still independent from θ and ϕ.

- The extended property d) and property e) enable one to use (30) for multiphoton radiation; this also holds in the case in which more than two charged particles are present in the final state.
- That is why, in the case of two-body decays (plus bremsstrahlung photons), such a type of phase-space treatment is sufficient for NLO precision.
- For NNLO precision, in matching of the two mappings for the collinear singularities[16] another factor of the type $\lambda^{1/2}(\dots)/\lambda^{1/2}(\dots)$ would have to be included in the W_n^{n+1} of (17) and (30). In fact, in such a case the exact multiphoton phase-space parametrization would be preserved.
- For each additional charged decay product present in the final state, still another factor of the type $\lambda^{1/2}(\dots)/\lambda^{1/2}(\dots)$ is needed in W_n^{n+1} to assure multichannel generation with the exact treatment of the phase-space.
- Even without future refinements (as explained in the previous two points) our phase-space parametrization is sufficient for NLO and NLL precision for the two-body (two-charges) decays, accompanied with an arbitrary number of photons. In the general case, when more than two charged particles are present in the final state, such a phase-space parametrization remains sufficient for LL only, even though also in this case the full multiphoton phase-space is covered. At present, the resulting precision is sufficient and does not justify those easy changes.
- In our choice of the phase-space parametrization (point 1), we have dropped some details, and the choice of the $\hat{x}$, $\hat{y}$ and $\hat{z}$ axes of the P rest frame were not specified. Indeed, for the decay of a scalar object, such as that discussed in the present paper, every choice is equivalent. In general, this is not the case. Already in the case of Z boson decay, the choice of the $\hat{z}$ axis parallel to the direction of the incoming beam of the same charge as k_2 is advantageous; see [14] where the process $e^+e^- \to Z \to l^+l^-n(\gamma)$ was studied. In this case the direction of the incoming beam coincides with the spin state of Z, and the choice simplifies the expression for the matrix element.
- Finally, we may consider extending our method beyond the decays. In the case of the t-channel processes, or initial state radiation, particular choices for the frames and angles would also be essential for the construction to match the structure of the matrix element singularities. Some hints in that direction can be seen already now [25, 26].

References

1. E. Barberio, B. van Eijk, Z. Was, Comput. Phys. Commun. **66**, 115 (1991)
2. E. Barberio, Z. Was, Comput. Phys. Commun. **79**, 291 (1994)
3. M. A. Dobbs et al., hep-ph/0403045
4. CDF Collaboration, V.M. Abazov et al., Phys. Rev. D **70**, 092 008 (2004)
5. OPAL Collaboration, G. Abbiendi et al., Phys. Lett. B **580**, 17 (2004)
6. DELPHI Collaboration, J. Abdallah et al., Eur. Phys. J. C **31**, 139 (2003)
7. NA48 Collaboration, A. Lai et al., Phys. Lett. B **602**, 41 (2004)
8. KTeV Collaboration, T. Alexopoulos et al., Phys. Rev. D **71**, 012 001 (2005)
9. Belle Collaboration, A. Limosani et al., hep-ex/0504046
10. BABAR Collaboration, B. Aubert et al., Phys. Rev. D **69**, 111 103 (2004)
11. FOCUS Collaboration, J.M. Link et al., hep-ex/0412034
12. P. Golonka, Z. Was, hep-ph/0508015
13. P. Golonka, Z. Was, Eur. Phys. J. C **45**, 97 (2006)
14. P. Golonka, Z. Was, hep-ph/0604232
15. A. Andonov et al., Comput. Phys. Commun. **174**, 481 (2006)
16. F. James, FOWL – a General Monte Carlo Phase Space Program, 1977, CERN Computer Centre Program Library, Long Writeup W505
17. T. Kinoshita, J. Math. Phys. **3**, 650 (1962)
18. T.D. Lee, M. Nauenberg, Phys. Rev. B **133**, 1549 (1964)
19. E. Baracchini, G. Isidori, Phys. Lett. B **633**, 309 (2006)
20. Z. Was, Written on the basis of lectures given at the 1993 European School of High Energy Physics, Zakopane, Poland, 12–25 September 1993
21. S. Jadach, Z. Was, R. Decker, J. H. Kuhn, Comput. Phys. Commun. **76**, 361 (1993)
22. A. Andonov, S. Jadach, G. Nanava, Z. Was, Acta Phys. Pol. B **34**, 2665 (2003)
23. G. Nanava, Z. Was, Acta Phys. Pol. B **34**, 4561 (2003)
24. S. Jadach, B.F.L. Ward, Z. Was, Phys. Rev. D **63**, 113 009 (2001)
25. Z. Was, Eur. Phys. J. C **44**, 489 (2005)
26. F.A. Berends, R. Kleiss, S. Jadach, Nucl. Phys. B **202**, 63 (1982)